Activation analysis of a compact Tokamak using Deuterium–Helium3 fuel

Fusion Engineering and Design 222 (2026) 115491

Contents lists available at ScienceDirect

Fusion Engineering and Design

journal homepage: www.elsevier.com/locate/fusengdes

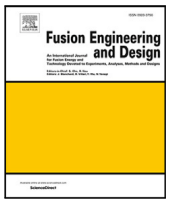

Activation analysis of a compact Tokamak using Deuterium–Helium3 fuel☆

A. Morandi*, D. Pettinari, M. Zucchetti

Department of Energy, Politecnico di Torino, Corso Duca degli Abruzzi 24, Torino, 10129, Italy

ARTICLE INFO

Keywords:
Deuterium-^{3}Helium fusion
Activation analysis
Compact tokamak
Neutronic analysis
Radioactive waste reduction
OpenMC
FISPACT-II
Fusion advanced fuels

ABSTRACT

Recent advancements in high-temperature superconducting (HTS) magnets have enabled tokamaks to reduce dimensions and operate with higher plasma parameters. This opens to the possibility of using advanced fuel mixtures such as Deuterium–^{3}Helium (DHe3). Compared to traditional fuels, DHe3 offers the potential to reduce neutron-induced activation and minimize the presence of tritium in the fuel cycle.

In a fusion reactor that uses a 50% Deuterium–50% ^{3}Helium mixture, neutrons are produced solely in the Deuterium–Deuterium (DD) and Deuterium–Tritium (DT) side reactions, while Tritium can be produced during DD reactions and is therefore absent at the startup of the machine.

This study proposes a comprehensive neutronic and activation analysis of a compact, high-field tokamak employing DHe3 fuel. Using OpenMC, an open-source Monte Carlo code, the feasibility and performance of this fuel mixture within the confines of a compact fusion reactor will be investigated. The activation analysis will be limited to the First Wall, Blanket and inboard Toroidal Field coils, with some simplifications in the tokamak layout.

By analyzing neutron interactions and activation processes, as well as design modifications, we seek to assess the potential benefits and challenges associated with implementing DHe3 as fuel.

1. Introduction

The deuterium–tritium (DT) fusion reaction is considered the most promising candidate for future fusion reactors because of its high cross section at relatively low temperatures and significant energy release, which facilitate ignition. However, it presents major issues related to safety and radioactive waste. The 14 MeV neutrons produced by the reaction require thick shields to protect personnel and sensitive materials, such as superconducting magnets. These neutrons can also activate materials, resulting in substantial amounts of low and medium-level radioactive waste.

Furthermore, tritium (T), unlike deuterium (D), is scarce and radioactive, making it a hazard to people and the environment. It is easily absorbed by materials and its decay hinders the possibility of storing large amounts of tritium for extended periods of time; this generates the necessity for efficient in situ breeding techniques to ensure self-sufficiency. With only about 35 kg of tritium available worldwide [1], future DT reactors must efficiently breed sufficient tritium to sustain continuous operation and support the startup of additional reactors. Achieving this requires careful consideration of numerous factors, including Tritium Breeding Ratios (TBR), material selection, Tritium Burning Efficiency (TBE) [2] and fuel cycle optimization [3].

Given the challenges associated with DT fusion, alternative fuel cycles could be investigated. One possible candidate is deuterium–^{3}helium (DHe3) fusion, as it produces fewer neutrons, reducing damage and activation. DHe3 fusion also decreases the tritium inventory, as tritium is mainly produced in one channel of the deuterium–deuterium (DD) side reaction and is quickly burnt due to its larger cross-section. Additionally, DHe3 generates 14.7 MeV protons, that could potentially be used for direct conversion to electricity [4]. Although DHe3 fusion offers significant advantages, it also introduces new obstacles, especially in meeting the demanding plasma conditions needed for ignition, which pose physical and engineering challenges. Moreover, ^{3}helium is scarce on Earth, and existing reserves, originating mainly from tritium decay and as a byproduct of natural gas extraction [5], are insufficient for large-scale energy production. Despite these obstacles, these challenges may be overcome in the future. Advancements in HTS magnets technology and may enable the higher plasma parameters necessary for DHe3 ignition. Looking forward, the integration of novel reactor designs and optimization strategies — such as spin-polarized fuels to boost fusion reaction rates [6], operating in the plasma's second stability region, and exploring direct energy conversion [4]— should be considered to enhance the feasibility of DHe3 fusion. Additionally,

☆ This article is part of a Special issue entitled: 'SOFT 2024' published in Fusion Engineering and Design.

* Corresponding author.
E-mail address: alessandro.morandi@polito.it (A. Morandi).

https://doi.org/10.1016/j.fusengdes.2025.115491
Received 21 January 2025; Received in revised form 13 June 2025; Accepted 7 October 2025
Available online 11 October 2025

research into extracting ^{3}He from lunar regolith, as explored in the ARTEMIS program [7], could mitigate resource scarcity issues.

This work is situated within this context, exploring how DHe3 fusion can be exploited to reduce the neutron flux in a high-field tokamak. The primary focus of this paper is to compare the performance, regarding material activation, of DT and DHe3 fuel mixtures, while also briefly addressing key challenges and advantages that could be considered in the implementation of this advanced fuel and suggesting potential steps that could be taken in future works.

The design considered in this study is an Affordable, Robust, Compact (ARC)-class tokamak, equipped with a 2LiF+BeF_2 (FLiBe) liquid immersion breeding blanket. This material provides efficient breeding, shielding and activation characteristics [8], but may present some problems regarding materials compatibility and costs. For these reasons, an alternative blanket configuration using borated water instead of FLiBe was examined. Borated water was chosen due to its neutron-absorbing properties and compatibility with existing technologies, making it a practical substitute for FLiBe in the case of DHe3 fuel. This configuration emphasizes the potential to eliminate the breeder blanket entirely, thereby simplifying reactor design while leveraging a more technologically established material.

Section 2 outlines the methodology followed to perform the neutronic analysis, executed on *OpenMC* [9], detailing the steps taken to develop a simplified CAD model of a compact tokamak along with the neutron source. The following sections describe the results derived from the neutronic analysis (Section 3) and the activation analysis carried out with *FISPACT-II* [10] (Section 4) respectively.

2. Setup for the neutronic analysis

2.1. Geometry and materials

This study considers parameters similar to the ARC (Affordable Robust Compact) tokamak – 2015 design [11] – in order to compare the results of the neutronic analysis with other studies done on a compact tokamak employing HTS magnet technology. While DHe3 presents unique challenges for tokamak designs, the ARC-class configuration was selected due to its innovative approach to compact, high-performance operation, making it an interesting choice for exploring advanced fuel cycles in magnetically confined systems.

The geometry was created using the Parametric "SingleNullSubmersionTokamak" available in the Paramak Python package [12] and taking dimensions similar to ARC. Paramak creates CadQuery objects that can be saved in various CAD files types and converted to Direct Accelerated Geometry Monte Carlo (DAGMC) h5m format, using the Cad-to_DAGMC tool [13].

The parameters used to create the selected geometry are summarized in Appendix, while Fig. 1 shows a cross-section of the reactor, as well as the materials used for the analysis; their composition is summarized in Table 1. The modeled geometry and materials represent a simplified version of an ARC-class tokamak. This simplification was made to reduce computational demands while retaining the key neutronic features necessary for a meaningful qualitative comparison.

More detailed geometries, including a refined radial build, may be explored in future studies to assess more complex activation patterns.

The volumes on which the neutron flux was calculated were:

- The **pure tungsten (W) First Wall**, that has a thickness of 7 cm and a volume of 15 m^3
- The **blanket made of FLiBe molten salt, or Borated Water** for the additional DHe3 simulation, has a volume of 278 m^3.
- The inner **Toroidal Field (TF) coil, made of YBCO** and with a volume of 37 m^3 (neglecting the top and bottom sections, that are part of the outboard TF coils). The superconducting magnets are modeled as being composed entirely of YBCO, with no inclusion of substrate or buffer layers. This represents a deliberate modeling assumption aimed at simplifying the analysis while preserving the main neutronic characteristics of the system.

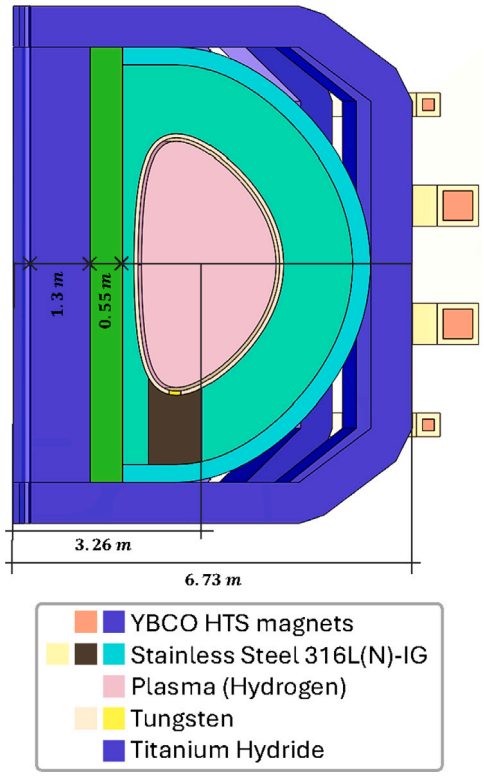

Fig. 1. Cross section of the geometry used for the analysis. Indicative dimensions are shown along the radial dimension. Materials are specified for each component, except for the blanket, that can be either FLiBe or Borated water. A more detailed description of the thicknesses of the layers can be found in Appendix.

These components were selected because they are the most critically exposed to neutron flux or, as in the case of the inboard TF coil, the effect of high neutron fluxes may be detrimental to their operation.

2.2. Definition of the source in OpenMC

The possible reaction types in a DT plasma (where the number in parenthesis represents the kinetic energy associated to each fusion products) are:

$$D + T \longrightarrow n\ (14.08\ MeV) + \alpha\ (3.52\ MeV)$$

$$D + D \longrightarrow p\ (3.02\ MeV) + T\ (1.01\ MeV)$$

$$D + D \longrightarrow n\ (2.45\ MeV) + {}^3He\ (0.82\ MeV)$$

The two DD reaction branches have nearly equal probability (~50%). In a DHe3 plasma the main reaction is:

$$D + {}^3He \longrightarrow \alpha\ (3.6\ MeV) + p\ (14.7\ MeV)$$

but also the aforementioned reactions for a DT plasma can occur. Other secondary reactions, such as TT, T^{3}He and ^{3}He^{3}He have not been considered in this study due to their significantly lower reactivity.

The formula used to calculate the fusion power resulting from the two different fuel mixtures is simply the sum of the energies of each fusion reaction (the two DD branches, DT or DHe3) multiplied by the respective reaction rate and weighted on the probability of each reaction occurring.

$$P_{fus} = \sum_i E_i \cdot p_i \cdot R_i$$

where E_i [J] is the energy of the reaction of type i, p_i [–] is the probability of the reaction of type i to occur, R_i [s^{-1}] is the reaction rate of the

Table 1
Materials used in the simulation. Weight percentage composition by element and density is also reported.

Material		Composition by element [weight %]	Density [g/cm^3]
HTS magnets (pure YBCO)		Y: 13.34, Ba: 41.23, Cu: 28.62 O: 16.81	6.3
SS316L(N)-IG (forged) [14]		C: 0.027, Mn: 1.67, Si: 0.34, P: 0.018, S: 0.001, Cr: 17.39, Ni: 12.35, Mo: 2.42, N: 0.072, Cu: 0.09, Ti: 0.009, Nb: 0.01, Ta: 0.009, Co: 0.02 Fe: 65.574	8.0
Tungsten		W: 100	19.3
Titanium Hydride (TiH_2)		Ti: 95.96, H: 4.04	3.75
FLiBe	Borated water 8000 ppm B solution [15]	H: 11.18, O: 88.72 B: 0.8 (95% B_{10} enriched)	1

reaction of type i, calculated using an average value for temperature and densities, and i can be either DT and DD (two channels) for a 50%D-50%T fuel mixture, or DHe3, DD (two channels) and DT for a 50%D-50%He3 fuel mixture.

To compare the performance of DHe3 fuel against DT, both were evaluated at a fusion power of 525 MW, as calculated in [11]. The average temperature and electron density chosen to achieve this power are:

- $T_{DT} = 15.3$ keV, $n_{e,DT} = 7 \cdot 10^{13}$ cm^{-3}
- $T_{DHe3} = 69$ keV, $n_{e,DHe3} = 1.3 \cdot 10^{14}$ cm^{-3}

This study did not examine the physical factors affecting plasma stability and ignition, as these will be addressed in future research. However, preliminary calculations indicate that the DHe3 plasma density approaches, but remains below, the Greenwald limit based on the parameters of the ARC reactor design.

One of the major obstacles in developing the model was establishing the DHe3 neutronic source. Although the primary reaction (D-He3) is inherently aneutronic, DD reactions have about a 50% chance of generating 2.45 MeV neutrons and 14.1 MeV neutrons are produced through DT reactions stemming from tritium formed by the other branch of DD reactions. In order to mimic this behavior, the reaction rates of DT and the two DD channels were set according to the thermal reactivities suggested in [16] and implemented in the *cfspopcon* Python package [17], while the DHe3 reaction rate was calculated following the derivation done in [18], considering a steady-state scenario and a tritium particle confinement time value of $\tau_T \sim 5$ s. This tentative value was chosen as a compromise between the value of $\tau_T = 23.5$ s used in [18] for ARIES-III, and a more conservative value comparable with the energy confinement time calculated for ARC in [11], $\tau_E = 0.64$ s. This figure serves as an approximation to incorporate realistic dynamics into the analysis, given that scaling laws for a DHe3 fuel mixture in a tokamak are not yet well established. Further studies are needed to define a more realistic neutronic source, both in the spatial and energy distribution.

An interesting point for future studies would be to examine the activation and damage effect of high energy protons generated by DHe3 fusions. If the protons have sufficiently large energies, they may escape the magnetic confinement. A preliminary calculation of their gyration radius, using the simple formula for the Larmor radius: $r_L = (m_p \cdot v_{th})/(q_p \cdot B)$, where m_p and q_p are the proton mass and charge, respectively, while v_{th} is the thermal velocity associated with the kinetic energy, can show how the 14.7 MeV protons should be safely confined in a high-field ($B = 9$ T) tokamak such as ARC, having a value of $r_L = 6$ cm, much smaller than the plasma chamber dimensions.

The simulations for both the fuel mixtures were carried out using over 10^9 particles run on a high-performance computing (HPC) system. Only neutrons were included in the simulations, as photon sources were not accounted for, and their inclusion would have significantly increased computational time.

TENDL-2019 [19] was the chosen nuclear data library used for the neutronic analysis.

The total neutron fluxes, summarized in Table 2, were obtained by normalizing the neutron tally calculated by *OpenMC*. This procedure is described in Chapter 8.3 of the *OpenMC* User's Guide.

3. Results of the neutronic analysis

This chapter presents the results of the neutronic analysis for three key components: the First Wall (FW), the Blanket, and the portion of the Toroidal Field (TF) coil located on the inboard side, hereafter referred to as the inner TF coils. The considered cases are: DT fuel with FLiBe blanket, DHe3 fuel with FLiBe blanket and DHe3 fuel with a borated water blanket.

It was calculated that in a DT fuel mixture, the average energy per fusion reaction, weighting the energies of DT and DD reactions on their probability of occurring, is 17.5 MeV and about 80.06% is carried by neutrons. In comparison, a DHe3 mixture produces slightly less energy per reaction at 16.4 MeV, but only 2.9% of its total energy is carried by neutrons. This shows how a DHe3 mixture can significantly reduce the neutron energy contribution compared to the DT mixture.

The analyses, summarized in Table 2, indicate that the use of DHe3 reduces the total neutron flux by at least an order of magnitude across all components, highlighting the primary advantage of this advanced fuel. Comparing the spectra for the two analyses carried out with a FliBe blanket, plotted in Fig. 3, it can be seen how the reduction is consistent throughout the energy spectrum, with the DT scenario having a prominent peak above the 10 MeV mark, due to the 14.1 MeV neutrons produced during the DT reactions. Conversely, the DHe3 scenarios display a more significant peak at approximately 2 MeV, due to a higher frequency of DD reactions, which generate 2.45 MeV neutrons.

As described in Section 1, the use of DHe3 fuel eliminates the necessity of breeding tritium. This permits the substitution of the FLiBe breeding blanket with a material that poses fewer technological challenges, serving solely as a coolant and ideally as a shield. Consequently, an informed choice in this regard was the substitution of the FLiBe blanket with borated water, widely used in the nuclear industry due to the high neutron capture cross-section of boron. Additional simulations demonstrated that this substitution does not significant alter the total neutron flux, that remains within the same order of magnitude for both DHe3 scenarios. This suggests that replacing the FLiBe blanket with borated water has a minimal impact on neutron flux levels. However, the neutron spectrum shows an increase in the slow neutron range (0.025 eV to 1 keV) on both the first wall and the blanket. This phenomenon can be attributed to the moderation effect of hydrogen atoms in water, which effectively slows down fast neutrons

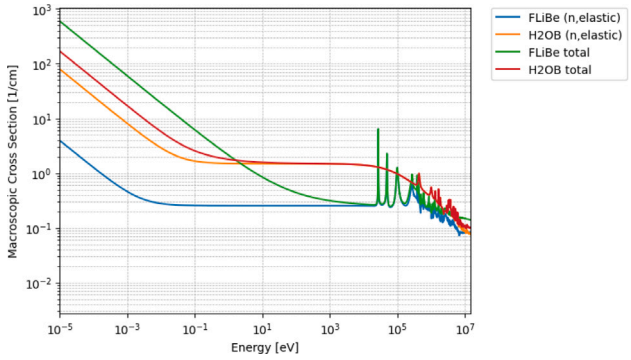

Fig. 2. Total and elastic scattering macroscopic cross sections cm^{-1} of borated water (H2OB) and FLiBe, obtained with the `plot_xs` function available in *OpenMC*, using the *TENDL-2019* nuclear data library.

Table 2
Neutrons per second and total neutron fluxes produced in each fuel mixture, averaged on the whole volume of the component. The upper rows report the relative contribution of main and secondary fusion reactions.

Fuel mixture (50–50)	DT	DHe3 (FLiBe)	DHe3 (H_2O+B)
DT %	99.46%	2.18%	2.18%
DDn %	0.28%	6.94%	6.94%
DDp %	0.26%	5.92%	5.92%
DHe3 %	0.0%	84.96%	84.96%
Neutrons per second	$1.91 \cdot 10^{20}$	$2.71 \cdot 10^{19}$	$2.71 \cdot 10^{19}$
Total flux on first wall [1/cm^2/s]	$9.94 \cdot 10^{14}$	$9.94 \cdot 10^{13}$	$7.56 \cdot 10^{13}$
Total flux on blanket [1/cm^2/s]	$5.14 \cdot 10^{13}$	$4.68 \cdot 10^{12}$	$1.32 \cdot 10^{12}$
Total flux on TF coil [1/cm^2/s]	$3.03 \cdot 10^{9}$	$1.04 \cdot 10^{8}$	$1.35 \cdot 10^{8}$

through elastic scattering (see Fig. 2). Although some of these slowed neutrons are absorbed by ^{10}B, the dominant effect is a net increase in backscattered thermal and epithermal neutrons returning to the wall, hence the elevated thermal-to-slow-neutron intensity seen in Fig. 3(a).

These results demonstrate the potential of DHe3 fuel to simplify reactor design by eliminating the need for a breeding blanket. However, fully realizing these benefits requires a reevaluation of the reactor configuration to optimize its advantages. In particular, while the use of borated water provides a level of neutron moderation and absorption, it may not be optimal as a standalone shielding solution. In particular, the use of borated water does not provide superior shielding compared to FLiBe, requiring careful balance between technological simplicity, cooling efficiency, and shielding effectiveness. Furthermore, while DHe3 offers certain design benefits, it presents greater challenges as a fusion reaction, which must be considered in conjunction with these trade-offs.

4. Activation analysis

The activation analysis of the selected reactor components is presented for exposure to two Full Power Years (FPY) of irradiation from either DT or DHe3 neutron source. This analysis reflects the expected operational lifespan of the vacuum vessel and blanket of the 2015 ARC reactor design [11]. The results obtained from this analysis should therefore be considered conservative, as a more realistic scenario would consist of cycles of irradiation and cooling phases.

It should also be underlined that the scope of this work is to provide a preliminary assessment of the advantages that the use of DHe3 may provide in terms of activation. The optimization of materials and geometry of the reactor is beyond the aims of this work and will be assessed in future studies.

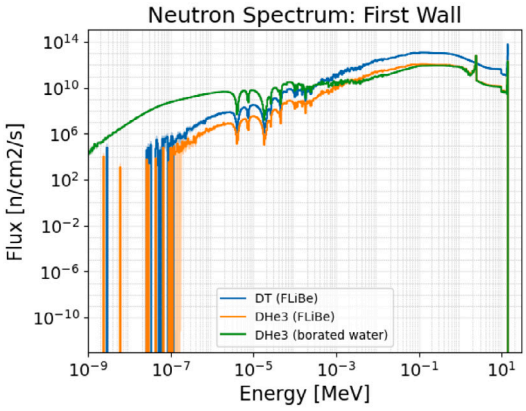

(a) Neutron spectra averaged on the whole First Wall for the three simulations considered

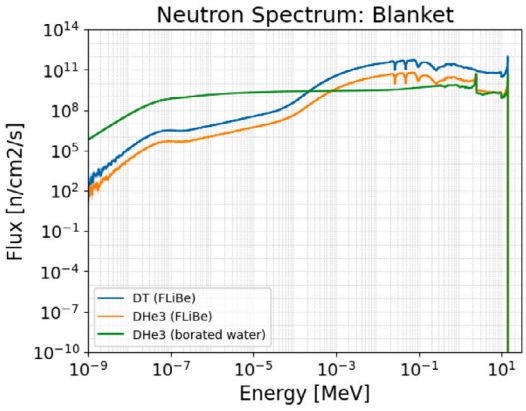

(b) Neutron spectra averaged on the whole Blanket for the three simulations considered

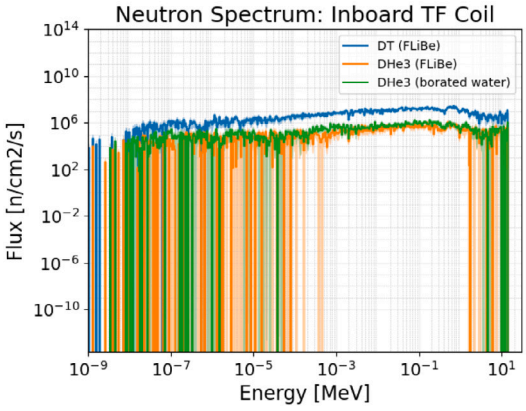

(c) Neutron spectra averaged on the whole inboard TF coil for the three simulations considered

Fig. 3. Neutron spectra of the three simulation types: DT with FLiBe blanket (blue), DHe3 with FLiBe blanket (orange) and DHe3 with borated water blanket (green) for the three components considered: First Wall (FW), Blanket and inboard Toroidal Field (TF) coils. The error is represented as a shaded area of the same color of the respective plot.

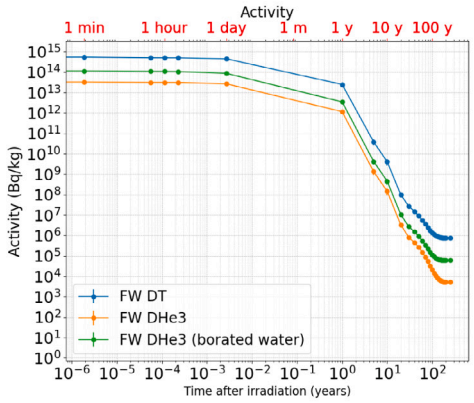

(a) Activity concentration [Bq/kg] averaged on the whole First Wall for the three simulations considered

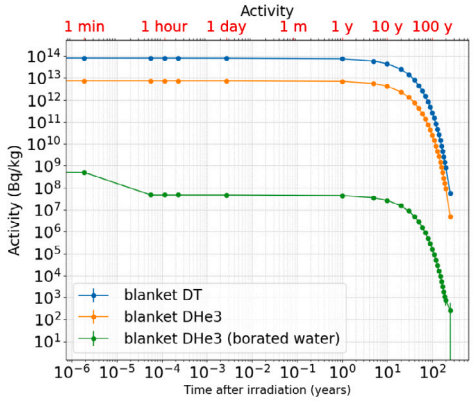

(b) Activity concentration [Bq/kg] averaged on the whole Blanket for the three simulations considered

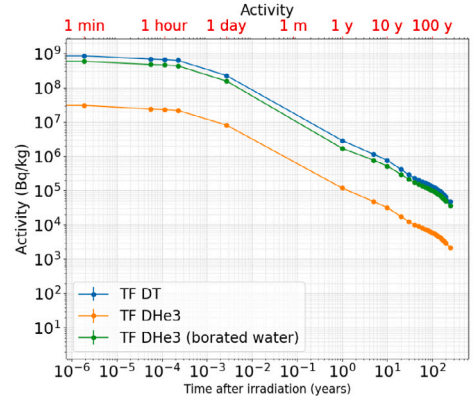

(c) Activity concentration [Bq/kg] averaged on the whole inboard TF coil for the three simulations considered

Fig. 4. Activity concentrations [Bq/kg] for: DT with FLiBe blanket (blue), DHe3 with FLiBe blanket (orange) and DHe3 with borated water blanket (green) for the three components considered.

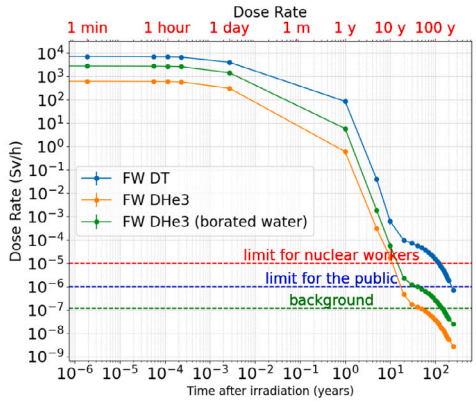

(a) Dose Rate [Sv/h] averaged on the whole First Wall for the three simulations considered

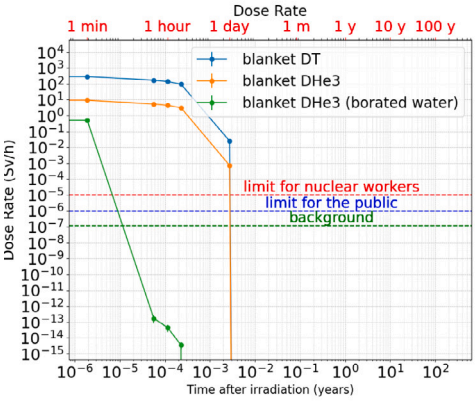

(b) Dose Rate [Sv/h] averaged on the whole Blanket for the three simulations considered

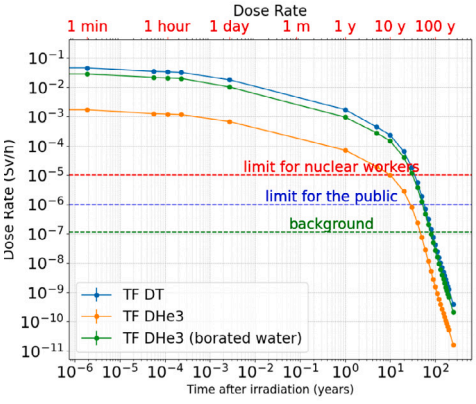

(c) Dose Rate [Sv/h] averaged on the whole inboard TF coil for the three simulations considered

Fig. 5. Dose Rates [Sv/h] for: DT with FLiBe blanket (blue), DHe3 with FLiBe blanket (orange) and DHe3 with borated water blanket (green) for the three components considered. Limits for nuclear workers, for the public and background radiation dose are showed with dashed lines.

The main inputs for the activation analysis on FISPACT-II, besides the irradiation time, are the total neutron flux, energy spectrum on each component and its composition in terms of elements before irradiation.

4.1. Reference dose limits for the activation analysis

The primary aim of employing DHe3 fuel is to reduce materials activation, thus minimizing radioactive waste, which in turn enhances the safety, the environmental impact but also the economic feasibility

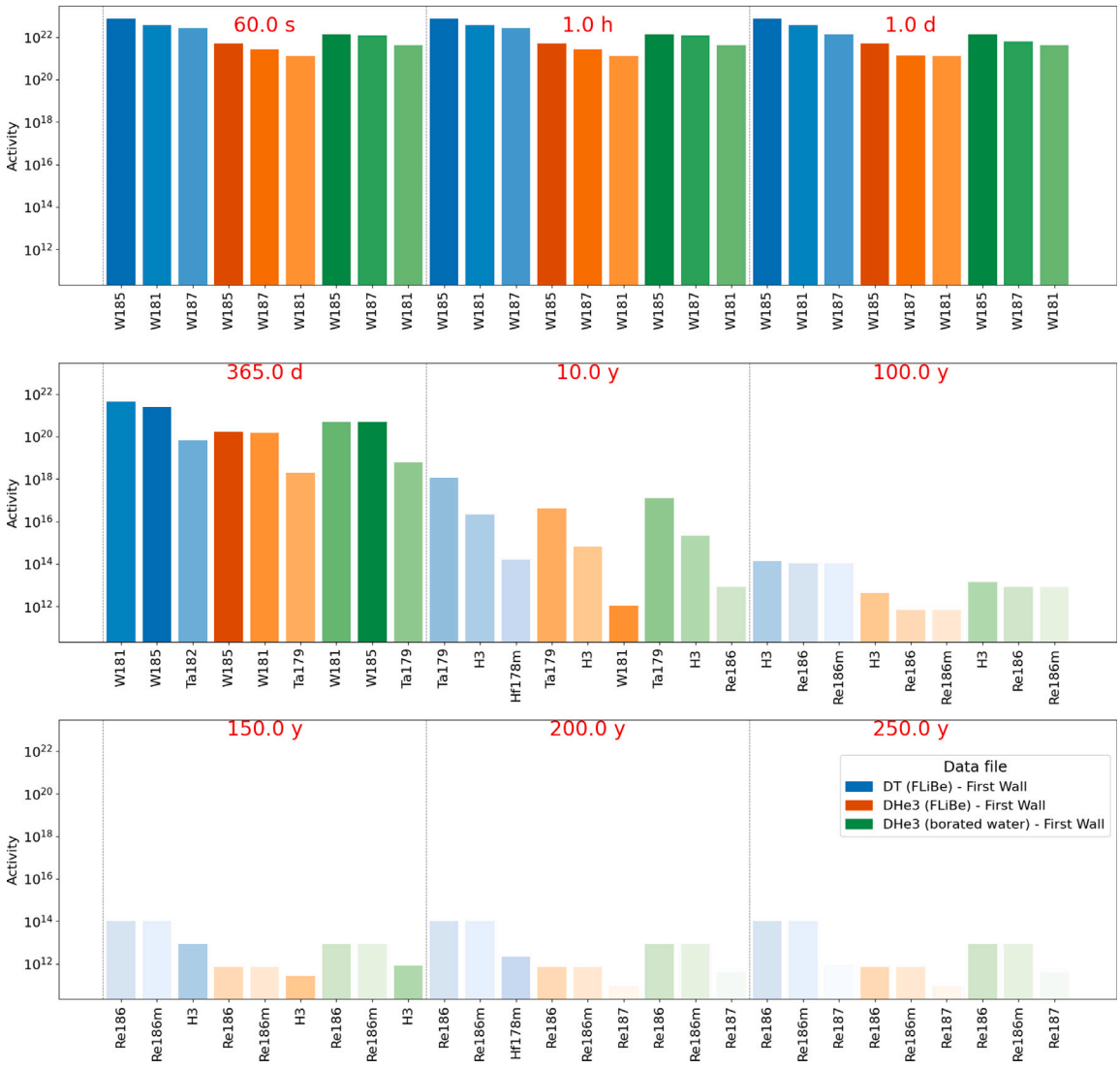

Fig. 6. Activity of the top three nuclides averaged on the whole first wall at selected timesteps for each of the three simulated scenarios.

of fusion reactors. Performance was measured against dose limits for nuclear workers and the public established by the ICRP [20].

In this study, the assessment of recycling criteria and the consideration of clearance of activated materials are not considered.

The annual dose limit for nuclear industry workers suggested by the ICRP is 20 mSv/y [20], or 10^{-5} Sv/h, considering constant exposure for 5 days a week in an 8-h workday. The dose limit for the public was set to 10^{-6} Sv/h, aligned with the limit of 1 mSv/y for non-nuclear employees and assuming continuous exposure during the working week. Furthermore, a dose rate of $2.74{\cdot}10^{-7}$ Sv/h was included for comparison with the average natural background dose worldwide of 2.4 mSv/y [21], assuming continuous exposure throughout the year.

4.2. Results of the activation analysis

Fig. 4 shows that the reduction in activity resulting from the use of DHe3 instead of DT is at least one order of magnitude for all components when a FLiBe blanket is taken into account. This outcome is consistent with the results of the neutronic analysis, as, if no other parameter concerning materials, irradiation time and energy spectrum is changed, the neutron flux is expected to be proportional to the activity. This can be simply explained by considering the activity as:

$$A = N\,\sigma\,\Phi\,(1 - e^{-\lambda t_a})\,e^{-\lambda t_w}$$

where:
N is the number of target atoms,
σ is the neutron cross section (cm^2),
Φ is the neutron flux ($n/cm^2/s$),
λ is the decay constant (s^{-1}),
t_a is the activation time (s) and t_w is the time between the end of activation and the start of the count.

Immediately after irradiation on the first Wall, the most dominant radioactive nuclides are all isotopes of tungsten. In particular W187, W185, W185m, W183m and W181 represent together more than 95% of the total activity in the DT case, and more than 99% in the two DHe3 cases.

After 10 years of cooldown the most dominant nuclide is tritium, representing more than 90% of the activity in all cases. The presence of tritium is most likely due to the W184(n,t) reaction with fast neutrons [22]. tritium stops being the highest contributor to the activity after about 100 years, when Re186 and Re186 m become dominant. Fig. 6 reports the three nuclides with the highest activity in the first wall during the cooldown phase.

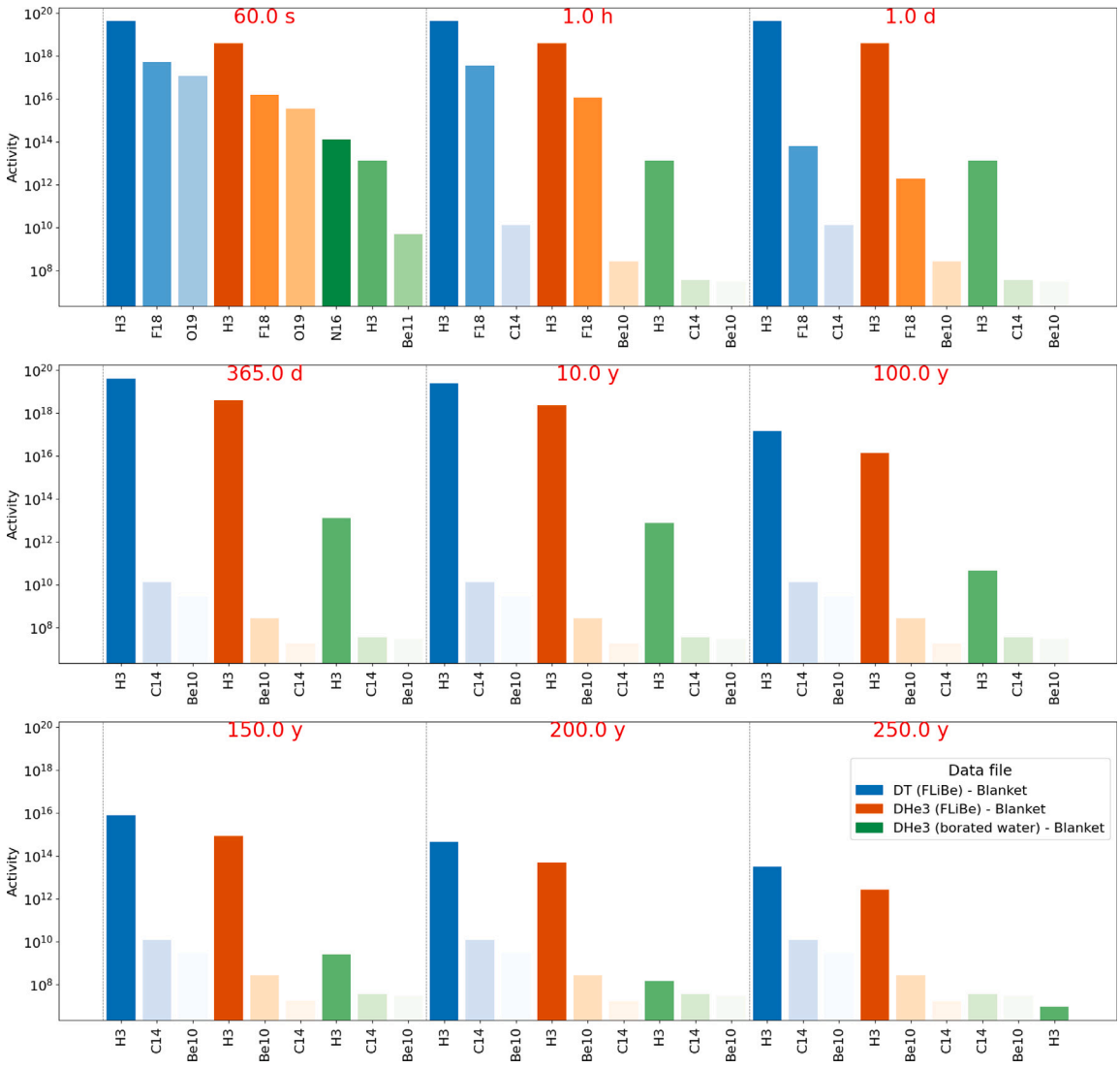

Fig. 7. Activity of the top three nuclides averaged on the whole blanket at selected timesteps for each of the three simulated scenarios.

The activity of the FLiBe blanket, shown in Fig. 4(b) is approximately one order of magnitude lower when using DHe3 instead of DT, as anticipated. Tritium is the main contributor to the activity throughout the entire cooldown period, as can be seen in Fig. 7. This is due to the neutron-induced tritium generation from Li6 (accounting for more than 99.9% of the production). In contrast, the use of a borated water blanket shows a significantly lower activation compared to the other cases. In this case, the dominant contributor to the activity is N16, a short-lived isotope of Nitrogen with a half-life of 7.13 s. However, its contribution to the total activity quickly becomes negligible with respect to tritium, that is present in lower amounts relative to the FLiBe blanket (see Fig. 4(b)).

The inboard toroidal field coil exhibits a significant presence of Cu64 during the initial days of cooldown. Over time, Y88, Co60 and Ba133 emerge as the most dominant nuclides, persisting up to approximately one year. In the long term, Ni63 and C14 become the primary contributors. This trend is shown in Fig. 8

Fig. 5 illustrates the total gamma dose rates calculated by FISPACT-II for the three types of simulation in the components examined. It can be immediately seen how the use of DHe3 can reduce the time required for activated components to fall below the aforementioned limits.

The DHe3 simulations consistently surpass DT in every scenario, achieving lower doses overall. Notably, DHe3 allows to reduce the dose rate on the FW (Fig. 5(a)) below the limit for nuclear workers in about 10 years, whereas DT needs at least 100.

The use of a borated water blanket, combined with the choice of DHe3 fuel mixture, outperforms DT as well. This highlights the importance of exploring innovative solutions to minimize waste in fusion devices while leveraging the unique advantages of DHe3.

5. Conclusions

This paper compares the performance of DT and DHe3 fuels in an ARC-class tokamak using a FLiBe immersion blanket, focusing on neutronic and activation characteristics. A simplified model for geometry, materials, and the neutron source was used. The findings highlight the significant advantages of DHe3 fuel, especially in reducing neutron production, material activation and the elimination of the need for tritium breeding. This simplifies the reactor design and may allow for a more compact system.

In this study, we showed that using DHe3 fuel at a temperature of 69 keV and an electron density of $1.3 \cdot 10^{14}$ cm^{-3} reduces the total neutron flux on the selected components (FW, Blanket and inboard TF coils) by at least one order of magnitude compared to DT fuel at 15.3 keV and $7 \cdot 10^{13}$ cm^{-3}. This reduction directly translates into a decrease

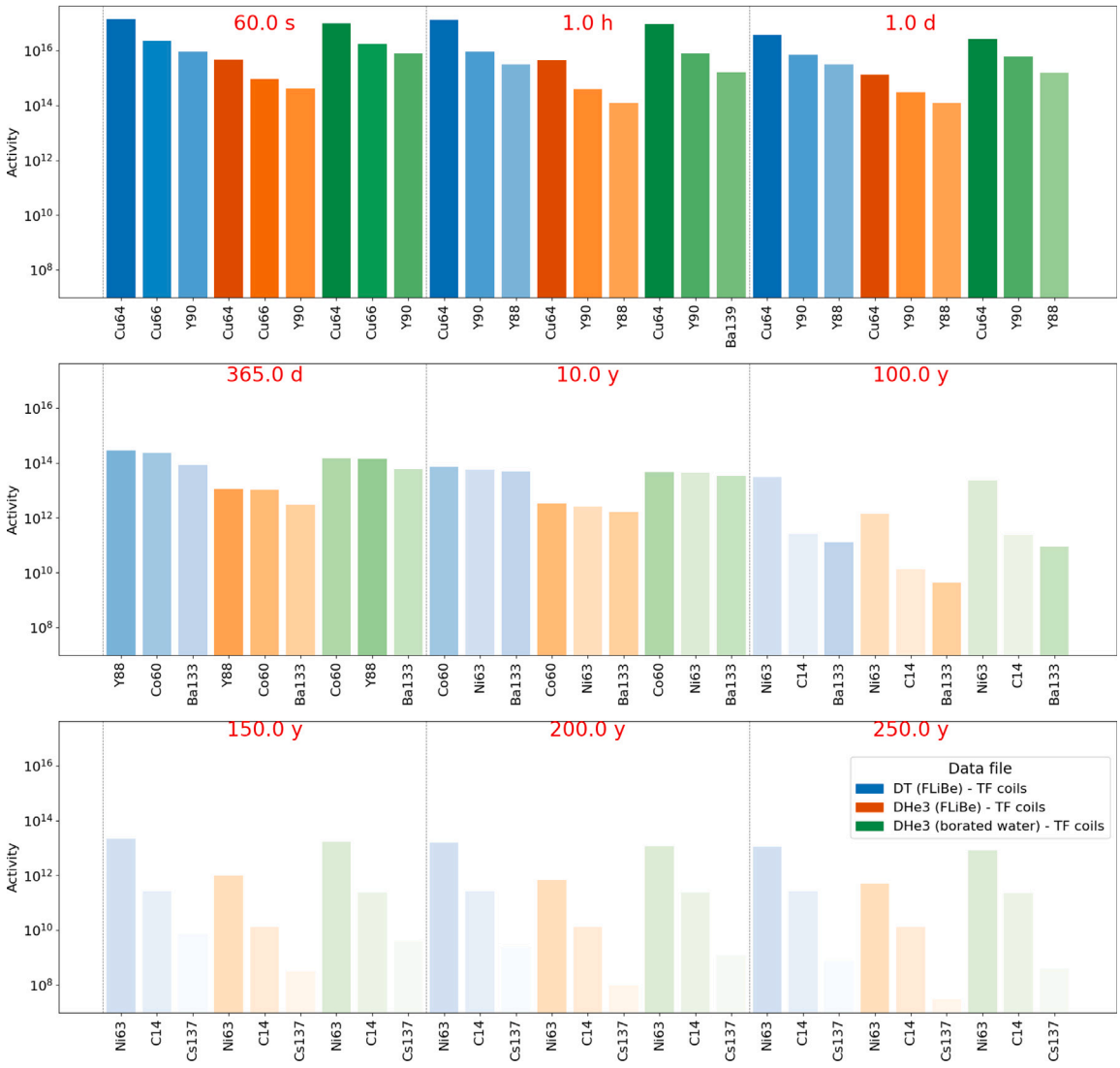

Fig. 8. Activity of the top three nuclides averaged on the whole inboard TF coil at selected timesteps for each of the three simulated scenarios.

in specific activity, allowing the dose rate to fall below regulatory limits more quickly. An additional DHe3 simulation has considered the substitution of the FLiBe blanket with borated water, since no breeding is necessary if this advanced fuel mixture is utilized. The selection of a less technologically challenging material, coupled with the use of DHe3 fuel, proved to be advantageous from the activation perspective, allowing a reduction of activation and contact dose on all the selected components with respect to the DT simulations.

Despite these advantages, significant challenges remain with DHe3 fuel. Achieving ignition is more complex compared to DT, ^{3}Helium is scarce on Earth, and DHe3 fusion technology and research is overall less developed than DT. Although the advantages of DHe3 fuel are evident, especially regarding safety and waste production, its economic and technical feasibility must also be rigorously evaluated. Future designs, building on concepts like ARIES-III [23], Apollo-L3 [24], Ignitor [25], and Candor [26], should incorporate recent technological breakthroughs, guiding the next generation of fusion reactors.

CRediT authorship contribution statement

A. Morandi: Writing – original draft, Methodology, Formal analysis, Conceptualization. **D. Pettinari:** Writing – review & editing, Methodology, Conceptualization. **M. Zucchetti:** Writing – review & editing, Supervision, Conceptualization.

Declaration of competing interest

The authors declare that they have no known competing financial interests or personal relationships that could have appeared to influence the work reported in this paper.

Acknowledgments

This publication is part of the project PNRR-NGEU which has received funding from the MUR – DM 352/2022 and DM 117/2023. Support from CINECA for high-performance computing is also acknowledged.

Appendix. Geometric parameters used in paramak

Table 3 reports the parameters used in Paramak to create the h5m geometry file.

Data availability

Data will be made available on request.

Table 3
Parameters used to create the "SingleNullSubmersionTokamak" in Paramak.

layer name	thickness [mm]
inner_bore_radial_thickness	300
inboard_tf_leg_radial_thickness	1000
center_column_shield_radial_thickness	550
divertor_radial_thickness	200
inner_plasma_gap_radial_thickness	60
plasma_radial_thickness	2260
outer_plasma_gap_radial_thickness	60
firstwall_radial_thickness	70
blanket_rear_wall_radial_thickness	300
number_of_tf_coils	18
support_radial_thickness	900
inboard_blanket_radial_thickness	188.7
outboard_blanket_radial_thickness	1163.2
elongation	1.84
triangularity	0.50
pf_coil_case_thicknesses	[100, 100, 100, 100]
pf_coil_radial_thicknesses	[200, 500, 500, 200]
pf_coil_vertical_thicknesses	[200, 500, 500, 200]
pf_coil_radial_position	[7000, 7500, 7500, 7000]
pf_coil_vertical_position	[2700, 1000, -1000, -2700]
rear_blanket_to_tf_gap	10
outboard_tf_coil_radial_thickness	700
outboard_tf_coil_poloidal_thickness	700
divertor_position	lower
support_position	lower
rotation_angle	90

References

[1] M. Kovari, M. Coleman, et al., Tritium resources available for fusion reactors, Nucl. Fusion 58 (2) (2017) 026010.

[2] D.G Whyte, R. Delaporte-Mathurin, et al., Tritium burn efficiency in deuterium–tritium magnetic fusion, Nucl. Fusion 63 (12) (2023) 126019.

[3] S. Meschini, S.E. Ferry, et al., Modeling and analysis of the tritium fuel cycle for ARC-and STEP-class DT fusion power plants, Nucl. Fusion 63 (12) (2023) 126005.

[4] D.R. Boris, Z. Ma, et al., Direct conversion of high energy protons to electricity using a solid-state pin junction diode, Fusion Sci. Technol. 52 (4) (2007) 1066–1069.

[5] Richard T. Kouzes, Azaree T. Lintereur, Edward R. Siciliano, Progress in alternative neutron detection to address the helium-3 shortage, Nucl. Instrum. Methods Phys. Res. Sect. A: Accel. Spectrometers Detect. Assoc. Equip. (ISSN: 0168-9002) 784 (2015) 172–175, http://dx.doi.org/10.1016/j.nima.2014.10.046, URL https://www.sciencedirect.com/science/article/pii/S0168900214012030. Symposium on Radiation Measurements and Applications 2014 (SORMA XV).

[6] J.F. Parisi, A. Diallo, J.A. Schwartz, Simultaneous enhancement of tritium burn efficiency and fusion power with low-tritium spin-polarized fuel, 2024, arXiv preprint arXiv:2406.05970.

[7] L.P. Keszthelyi, J.A. Coyan, et al., Assessment of Lunar Resource Exploration in 2022, Technical Report, US Geological Survey, 2023.

[8] S. Segantin, R. Testoni, M. Zucchetti, Neutronic comparison of liquid breeders for ARC-like reactor blankets, Fusion Eng. Des. (ISSN: 0920-3796) 160 (2020) 112013, http://dx.doi.org/10.1016/j.fusengdes.2020.112013, URL https://www.sciencedirect.com/science/article/pii/S0920379620305615.

[9] P.K. Romano, N.E. Horelik, et al., OpenMC: A state-of-the-art Monte Carlo code for research and development, Ann. Nucl. Energy (ISSN: 0306-4549) 82 (2015) 90–97, http://dx.doi.org/10.1016/j.anucene.2014.07.048, Joint International Conference on Supercomputing in Nuclear Applications and Monte Carlo 2013, SNA + MC 2013. Pluri- and Trans-disciplinarity, Towards New Modeling and Numerical Simulation Paradigms.

[10] J.-Ch. Sublet, J.W. Eastwood, et al., FISPACT-II: An advanced simulation system for activation, transmutation and material modelling, Nucl. Data Sheets (ISSN: 0090-3752) 139 (2017) 77–137, http://dx.doi.org/10.1016/j.nds.2017.01.002, Special Issue on Nuclear Reaction Data.

[11] B.N. Sorbom, J. Ball, et al., ARC: A compact, high-field, fusion nuclear science facility and demonstration power plant with demountable magnets, Fusion Eng. Des. 100 (2015) 378–405.

[12] J. Shimwell, J. Billingsley, et al., The paramak: Automated parametric geometry construction for fusion reactor designs, F1000Research (2021) http://dx.doi.org/10.12688/f1000research.28224.1.

[13] J. Shimwell, CAD to DAGMC. Convert CAD geometry (STP files) or cadquery assemblies to DAGMC h5m files, 2024, URL https://github.com/fusion-energy/cad_to_dagmc.

[14] G.W Wille, K.T Slattery, et al., Development of 316L(N)-IG stainless steel fabrication approaches for ITER divertor and limiter applications, Fusion Eng. Des. (ISSN: 0920-3796) 39–40 (1998) 499–504, http://dx.doi.org/10.1016/S0920-3796(98)00138-0.

[15] C. Gasparrini, D. Badocco, L. Di Pace, N. Terranova, P. Pastore, F. Montagner, L. Mattarozzi, R. Villari, E. Martelli, S. Roccella, et al., Water chemistry in fusion cooling systems: Borated water for DTT vacuum vessel, IEEE Trans. Plasma Sci. 50 (11) (2022) 4287–4291.

[16] H.S. Bosch, G.M. Hale, Improved formulas for fusion cross-sections and thermal reactivities, Nucl. Fusion 32 (4) (1992) 611, http://dx.doi.org/10.1088/0029-5515/32/4/I07.

[17] CFSpopcon repository on GitHub, cfspopcon: 0D Plasma Calculations & Plasma OPerating CONtours, URL https://github.com/cfs-energy/cfspopcon/tree/6050f4a541cd5c04c41ba35c6a0cea8816e72fe4. GitHub repository.

[18] E. Pedretti, S. Rollet, Comparison of neutronic productions during operation of the Aries-III second stability D^3He tokamak reactor without and with tritium-assisted startup, in: Emerging Nuclear Energy Systems: Icenes' 93 - Proceedings of the Seventh International Conference, World Scientific, 1994, p. 47.

[19] A.J. Koning, D. Rochman, et al., TENDL: Complete nuclear data library for innovative nuclear science and technology, Nucl. Data Sheets (ISSN: 0090-3752) 155 (2019) 1–55, http://dx.doi.org/10.1016/j.nds.2019.01.002, Special Issue on Nuclear Reaction Data.

[20] ICRP, The 2007 Recommendations of the International Commission on Radiological Protection, vol. 37, ICRP Publication 103. Ann. ICRP, 2007, (2-4).

[21] United Nations Scientific Committee on the Effects of Atomic Radiation and others, Sources and Effects of Ionizing Radiation, United Nations Scientific Committee on the Effects of Atomic Radiation (UNSCEAR) 2008 Report, Volume I: Report to the General Assembly, with Scientific Annexes a and B-Sources, United Nations, 2010.

[22] N. Soppera, M. Bossant, E. Dupont, JANIS 4: An improved version of the NEA java-based nuclear data information system, Nucl. Data Sheets (ISSN: 0090-3752) 120 (2014) 294–296, http://dx.doi.org/10.1016/j.nds.2014.07.071.

[23] J.F. Santarius, J.P. Blanchard, et al., Energy conversion options for ARIES-III - a conceptual D^3He tokamak reactor, in: IEEE Thirteenth Symposium on Fusion Engineering, IEEE, 1989, pp. 1039–1042.

[24] G.L. Kulcinski, J.P. Blanchard, et al., Summary of APOLLO, a D-3he tokamak reactor design, Fusion Technol. 21 (4) (1992) 2292–2296.

[25] B. Coppi, A. Airoldi, et al., Perspectives for the high field approach in fusion research and advances within the ignitor program, Nucl. Fusion 55 (5) (2015) 053011.

[26] B. Coppi, Physics of neutronless fusion reacting plasmas, Phys. Scr. 1982 (T2B) (1982) 590.